Mon. Not. R. Astron. Soc. **345,** 480–496 (2003)

A homogeneous sample of sub-damped Lyman α systems – II. Statistical, kinematic and chemical properties

Céline Péroux,[1,2★†] Miroslava Dessauges-Zavadsky,[3,4] Sandro D'Odorico,[3] Tae-Sun Kim[3,2] and Richard G. McMahon[2]

[1] *Osservatorio Astronomico di Trieste, Via G. B. Tiepolo 11, 34131 Trieste, Italy*
[2] *Institute of Astronomy, Madingley Road, Cambridge CB3 0HA*
[3] *European Southern Observatory, Karl-Schwarzchild-Str. 2, 85748 Garching bei München, Germany*
[4] *Observatoire de Genève, 1290 Sauverny, Switzerland*

Accepted 2003 June 26. Received 2003 May 9; in original form 2002 December 6

ABSTRACT

Damped Lyman α systems (DLAs), with $N(\mathrm{H\,I}) > 2 \times 10^{20}$ atom cm^{-2}, observed in the spectra of quasars have allowed us to quantify the chemical content of the Universe over cosmological scales. Such studies can be extended to lower column densities, in the sub-DLA range [$10^{19} < N(\mathrm{H\,I}) < 2 \times 10^{20}$ atom cm^{-2}], which are systems believed to contain a large fraction of the neutral hydrogen at $z > 3.5$. In this paper, we use a homogeneous sample of sub-DLAs from the European Southern Oberservatory (ESO) Ultraviolet–Visual Echelle Spectrograph (UVES) archives presented in Paper I, to determine observationally for the first time the shape of the column density distribution, $f(N)$, down to $N(\mathrm{H\,I}) = 10^{19}$ atom cm^{-2}. The results are in good agreement with the predictions from Péroux et al. We also present the kinematic and clustering properties of this survey of sub-DLAs, which appear to be marginally different from the DLAs. We compare low- and high-ionization transition widths and find that the properties of the sub-DLAs span roughly the parameter space of DLAs. We also find hints of an increase of metallicity in systems with larger velocity widths in the metal lines, although the statistical significance of this result is low.

Then we analyse the chemical content of this sample in conjunction with a compilation of abundances from 72 DLAs taken from the literature. As previously reported, the individual metallicities traced by [Fe/H] of these systems evolve mildly with redshift. Moreover, we analyse the H I column-density-weighted mean abundance, which is believed to be an indicator of the metallicity of the Universe. Although the number statistics is limited in the current sample, the results suggest a slightly stronger evolution of this quantity in the sub-DLA range. The effect is predominant at $z < 2$ and most of the evolution observed lies in this redshift range. Observational arguments support the hypothesis that the evolution we probe in the sub-DLA range is *not* due to their lower dust content. Therefore, these systems might be associated with a different class of objects, which better trace the overall chemical evolution of the Universe. Finally, we present abundance ratios of [Si/Fe], [O/Fe], [C/Fe] and [Al/Fe] for sub-DLAs in conjunction with DLA measurements from the literature. The elemental ratios in sub-DLAs are comparable with those from DLAs. It is difficult to decipher whether the observed values are the effect of nucleosynthesis or are due to differential dust depletion. The metallicities are compared with two different sets of models of galaxy evolution in order to provide constraints on the morphology of quasar absorbers.

Key words: galaxies: abundances – galaxies: evolution – galaxies: formation – galaxies: high-redshift – quasars: absorption lines – quasars: general.

★E-mail: peroux@ts.astro.it
†Marie Curie Fellow

1 INTRODUCTION

In addition to traditional emission studies, absorption systems along the line of sight to distant quasars provide a completely independent probe of galaxy evolution. The highest column density damped Lyα systems (hereafter DLAs) have $N(\mathrm{H\,I}) > 2 \times 10^{20}$ atom cm^{-2}. The reason why damped systems are a cosmologically important population is that they contain most of the neutral gas in the Universe at $z > 1$ (Lanzetta et al. 1991; Wolfe et al. 1995; Storrie-Lombardi, McMahon & Irwin 1996b). Since the metal content of these systems can be determined with rather high precision up to high redshift, they are a powerful tool for studying the chemical evolution of galaxies. In particular, a way to trace the metallicity of the Universe is provided by estimating the ratio of the total metal content to the total gas content measured in these systems (Pettini et al. 1997; Pei, Fall & Hauser 1999). Using such techniques, Prochaska & Wolfe (2002), in agreement with previous work, find that the hydrogen column-density-weighted [Fe/H] metallicities have similar values from $1.5 < z < 3.5$. The results are in disagreement with expectations since models of cosmic chemical evolution (e.g. Pei & Fall 1995) predict evolution of global metallicity with cosmic time. Savaglio (2000), however, has used 50 DLAs and lower column density systems and finds clear evidence for redshift evolution, although this sample suffers high inhomogeneity.

In a recent study, Péroux et al. (2003) have shown that sub-DLAs, defined as systems with $10^{19} < N(\mathrm{H\,I}) < 2 \times 10^{20}$ atom cm^{-2}, play a major role, especially at higher redshifts. The authors postulate that at $z > 3.5$, 45 per cent of the neutral gas mass is in sub-DLAs. These predictions are based on a constrained extrapolation of the quasar absorber column density distribution, $f(N)$, to lower column densities, assuming the distribution can be fitted by a gamma function. This suggests that the metallicities of sub-DLAs require detailed study in order to obtain a complete picture of the redshift evolution of the metallicity of the Universe. For this purpose, we have constructed a homogeneous sample of sub-DLAs based on high-resolution quasar spectra from the ESO UVES/VLT archives (Dessauges-Zavadsky et at. 2003, hereafter Paper I). Sub-DLAs can be easily picked up since at these column densities damping wings are already formed and the rest equivalent width is $W_{\mathrm{rest}} > 2.5$ Å.

In this paper, we analyse the sample of sub-DLAs presented in Paper I. We first use these data to establish the column density distribution in a range unprobed previously. These results have direct implications for the determination of the neutral gas content of quasar absorbers and their evolution with redshift. We also emphasize the limitations of the present sample in terms of the redshift path surveyed. The clustering properties of our sample of sub-DLAs are described in Section 3. In Section 4, we discuss the kinematic properties of the low- and high-ionization transitions associated with the sub-DLAs presented in Paper I. These results can be used to directly constrain some of the semi-analytic models recently presented in the literature. In Section 5, we present the results of chemical abundance determinations in sub-DLAs in conjunction with the abundances in DLAs taken from the literature and provide information on the global metallicity evolution of both individual quasar absorbers and the Universe. We also cross-correlate these properties with the kinematic information we present in previous sections. Relative abundances are then analysed and compared with recent models of galaxy formation and evolution, putting further constraints on the morphology of quasar absorbers.

2 STATISTICAL PROPERTIES OF SUB-DLAS

2.1 Sample definition

The sample of quasars used for this study is presented in Paper I and their characteristics are summarized in Table 1. This led to a set of 22 quasars studied in various observational programmes. In order to build the 'statistical sample', we have ignored the quasars that have been targeted for the study of the Lyα forest (for the analysis of voids, low column density column density distribution, etc.). Indeed, these have been *pre-selected* for not having Lyman limit systems (LLS) in their spectrum, precisely the type of feature we are looking for in the present study. As reported in Paper I, a sub-DLA at $z_{\mathrm{abs}} = 1.838$ was found in Q1101−264, a quasar observed during UVES Science Verification. This absorber is included in the abundance analysis, although for consistency, neither the redshift path of the quasar nor the sub-DLA are used in the 'statistical sample'. This selection process resulted in a sample of 21 quasars suitable for studying the statistical properties of sub-DLAs.

Similarly, sub-DLAs which do not have their Lyα feature within the spectral coverage are automatically excluded, although the determination of H I column density might be possible from other lines of the Lyman series. This is the case of the sub-DLA at $z_{\mathrm{abs}} = 3.171$ towards Q1451+123, for which we undertook a detailed abundance study similar to the other systems, but which is not included in our 'statistical sample'. The resulting sample of sub-DLAs is thus composed of 10 systems. Although we looked for any system with $N(\mathrm{H\,I}) > 10^{19}$ atom cm^{-2}, the smallest column density sub-DLA detected in this sample is $N(\mathrm{H\,I}) = 10^{19.32}$ atom cm^{-2}.

The large majority of the quasars in the sample were observed with UVES because there was a DLA along their line of sight, as can be attested from Table 1. There is no a priori reason for this to create a bias for our statistical analysis.

Table 1 lists the minimum (z_{min}) and maximum (z_{max}) redshifts along which a sub-DLA could be detected along each quasar line of sight. z_{min} corresponds to the point where the signal-to-noise ratio was too low to find absorption features at the sub-DLA threshold of $W_{\mathrm{rest}} = 2.5$ Å, and z_{max} is 3000 km s^{-1} blueward of the Lyα emission of the quasar. We took care to exclude the DLA regions and the gaps in the spectrum due to non-overlapping settings when computing the redshift path surveyed.

2.2 Number density

The number density of quasar absorbers is the number of absorbers, n, per unit redshift dz, i.e. $\mathrm{d}n/\mathrm{d}z = n(z)$. d$z$ is computed by summing up the redshift paths surveyed along the line of sight of each of the quasars studied as given in Table 1. $n(z)$ is a directly observable quantity, although, its interpretation is dependent on the geometry of the Universe. Indeed, the evolution of the number density of absorbers with redshift is the intrinsic evolution of the true number of absorbers combined with effects due to the expansion of the Universe.

Measuring the incidence of sub-DLAs down to $N(\mathrm{H\,I}) = 10^{19}$ atom cm^{-2} in a given sample of quasars requires a number of high-resolution spectra in order to unambiguously select all the absorption systems. Nevertheless, indirect information is also provided by the number of LLSs in a given quasar sample. Péroux et al. (2003) fitted the observed cumulative number of absorbers of both DLAs and LLSs with a Γ-distribution as suggested by Pei & Fall (1995) and first implemented by Storrie-Lombardi, Irwin & McMahon (1996a).

Table 1. dz covered by each quasar used from the UVES archives and the associated sub-DLA systems.

Quasar Name	z_{em}	Lyα forest coverage ($z_{min} - z_{max}$)[a]	z_{DLA}	$z_{sub\text{-}DLA}$	Sub-DLA N(H I)
Q0000−2620	4.11	2.533–3.365 and 3.423–4.105	3.390	...	...
BR J0307−4945	4.75	3.119–3.903 and 4.034–4.455	4.466	...	...
...	...	and 4.482–4.774	...	...	...
Q0347−3819	3.23	2.017–3.014	3.025	...	...
Q0841+129	2.50	1.903–2.362 and 2.387–2.466	2.375	...	...
...	...	and 2.484–2.497	2.476	...	...
HE 0940−1050	3.05	1.719–2.183 and 2.933–3.046	...	...	...
Q1038−272	2.32	2.107–2.357	...	...	...
Q1101−264[b]	2.14	1.519–2.117	...	1.838[b]	19.50 ± 0.05
HE 1104 − 1805[c]	2.31	1.609–1.654 and 1.670–2.307	1.662	...	...
Q1151+068	2.76	1.797–2.756	1.774[d]	...	...
PKS 1157+014	1.99	1.559–1.918 and 1.982–1.987	1.44	...	...
Q1223+1753	2.94	2.044–2.446 and 2.484–2.936	2.466	2.557	19.32 ± 0.15
PKS 1232+0815	2.57	1.704–2.327 and 2.350–2.566	2.338	...	...
Q1409+095	2.86	2.126–2.448 and 2.463–2.856	2.456	2.668	19.75 ± 0.10
Q1444+014	2.21	1.710–2.082 and 2.091–2.207	...	2.087	20.18 ± 0.10
Q1451+123	3.25	2.168–2.462 and 2.475–2.995	2.469	3.171[e]	19.70 ± 0.15
...	...	...	2.255	...	...
Q1511+090	2.88	1.720–2.876	...	2.088	19.47 ± 0.10
Q2059−360	3.09	2.461–3.068	3.083	2.507	20.21 ± 0.10
Q2116−358	2.34	1.710–1.992 and 2.000–2.337	...	1.996	20.06 ± 0.10
Q2132−433	2.42	1.710–1.907 and 1.923–2.417	1.914	...	...
PSS J2155+1358	4.26	2.913–3.300 and 3.337–3.606	3.316	3.142	19.94 ± 0.10
...	...	and 3.689–4.255	...	3.565	19.37 ± 0.15
...	...	...	...	4.212	19.61 ± 0.15
Q2206−199	2.56	1.720–1.914 and 1.917–2.071	1.920	...	...
...	...	and 2.083–2.556	2.076	...	...
PSS J2344+0342	4.24	2.889–3.201 and 3.241–3.606	3.220	3.882	19.50 ± 0.10
...	...	and 3.689–4.295	...	...	...

[a] z_{min} corresponds to the point where the signal-to-noise ratio was too poor to find absorption features and z_{max} is 3000 km s^{-1} bluewards of the Lyα emission of the quasar. The holes in the redshift intervals correspond to either a DLA or a gap in the spectrum due to non-overlapping settings.

[b] This quasar has been observed as part as the Science Verification of UVES for the study of the Lyα forest. As such, it does not fulfil our criteria for its redshift path to be included in our 'statistical sample'. Nevertheless, an analysis of the spectrum reveals the presence of a sub-DLA system at $z_{abs} = 1.838$ and we undertook the determination of the abundance of this absorber.

[c] This quasar is gravitationally lensed. Only the brightest line of sight was included in our study.

[d] This system is situated outside our spectral coverage.

[e] Our spectrum does not cover the Lyα line of this sub-DLA ($z_{abs} = 3.171$, $\lambda_{obs} \sim 5070$ Å). It has been identified thanks to the H I column density measurement reported by Bechtold (1994) and Petitjean, Srianand & Ledoux (2000). Several lines from the Lyman series and metals are available, hence, we undertook the determination of the metal content of this system but did not include it in our 'statistical sample'.

This puts constraints on the number of systems in the $10^{19} < N$(H I) $< 2 \times 10^{20}$ atom cm^{-2} column density range. They then used these predictions to compute the expected number density of sub-DLAs. The results from this work are tabulated in the last column of Table 2 for comparison with the observations presented here.

Excluding Q1101−264, we have sampled a total redshift path d$z = 17.5$ and find a total of 10 sub-DLAs. The comparison with the predictions of Péroux et al. (2003) show a good agreement in the intermediate redshift range. At $z > 3.5$, the low number statistics makes the results more uncertain. Nevertheless, it is important to note that in the quasar sample studied here all but four of the objects have $z_{em} < 3.5$. The sub-DLAs are thus predominantly located in the intermediate redshift range $2 < z_{abs} < 3.5$. Indeed, we find seven sub-DLAs at $z_{abs} < 3.5$, where we have surveyed d$z = 14.4$, while we find three sub-DLAs at $z_{abs} \gtrsim 3.5$, where we have only surveyed d$z = 3.1$. Consequently, the determination of $n(z)$ at $z_{abs} \gtrsim 3.5$ is not possible with the current set of data. The number of sub-DLAs and associated redshift paths are summarized in Table 2 for various redshift ranges.

2.3 Column density distribution

2.3.1 Observationally constraining f(N) down to log N(H I) = 19.0

Our sample of sub-DLAs from the UVES archive quasar spectra can be further used to determine the column density distribution of absorbers in the column density range $10^{19} < N$(H I) $< 2 \times 10^{20}$ atom cm^{-2}. The column density distribution describes the evolution of quasar absorbers as a function of column density. It is defined as

$$f(N, z)\,\mathrm{d}N\,\mathrm{d}X = \frac{n}{\Delta N \sum_{i=1}^{m} \Delta X_i}\,\mathrm{d}N\,\mathrm{d}X, \quad (1)$$

where n is the number of quasar absorbers observed in a column density bin $[N, N + \Delta N]$ obtained from the observation of m

Table 2. This table gives the redshift path surveyed, dz, and corresponding physical distance interval, dX (in a $\Omega_M = 0.3$, $\Omega_\Lambda = 0.7$ cosmology) for various redshift ranges. The observed number density of sub-DLAs is from our 'statistical sample' of 21 quasars from the UVES archive spectra. The predicted number density is from Péroux et al. (2002) who used a fit to the observed number of DLAs with an additional constraint from the total number of LLS.

z range	dz obs	dX obs	Number of sub-DLAs	$n(z)$ obs	$n(z)$ predicted
<3.5	14.4	47.0	7	0.49	0.46
>3.5	3.1	12.5	3	0.97	1.66
1.5–2.5	8.7	27.0	3	0.34	0.39
2.5–3.0	3.8	13.0	3	0.79	0.46
3.0–3.5	1.9	7.0	1	0.53	0.67
3.5–4.0	1.7	6.8	2	1.18	1.52
4.0–5.0	1.4	5.7	1	0.71	2.00
Total	17.5	59.5	10	0.57	0.58

quasar spectra with total absorption distance coverage $\sum_{i=1}^{m} \Delta X_i$. The distance interval, dX, is used to correct to comoving coordinates and thus depends on the geometry of the Universe. For a non-zero Λ-Universe:

$$X(z) = \int_0^z (1+z)^2 \left[(1+z)^2(1+z\Omega_M) - z(2+z)\Omega_\Lambda\right]^{-1/2} \mathrm{d}z. \quad (2)$$

The values of dX used in our study are given in Table 2 for an $\Omega_M = 0.3$, $\Omega_\Lambda = 0.7$ cosmology. We have sampled a total redshift path of d$z = 17.5$. This corresponds to a distance interval of dX = 59.5 in the $\Omega_M = 0.3$, $\Omega_\Lambda = 0.7$ cosmological model.

We have used the sample of sub-DLAs from the UVES archive quasar spectra to determine the column density distribution down to $N(\mathrm{H\ I}) = 10^{19}$ atom cm^{-2} for the first time. The results are shown in Fig. 1 together with the predictions of Péroux et al. (2002) computed from the expected number of sub-DLAs and a compilation of DLAs at all redshifts. The observational results presented here are consistent with the predicted change of slope of the column density distribution at $N(\mathrm{H\ I}) \sim 10^{19}$ atom cm^{-2}, as suggested by previous work (Petitjean et al. 1993; Storrie-Lombardi & Wolfe 2000; Péroux et al. 2003). This feature is probably the signature of the onset of self-shielding in these systems.

2.3.2 *Comparison with models*

Although simulating high column density systems such as DLAs is still extremely challenging because of resolution limitations, Gardner et al. (1997) have tried to overcome the problem by imposing the density profile of resolved haloes on to unresolved ones. They derive the evolution with redshift of the column density distribution and, interestingly, they find a flattening of the distribution somewhere in the region $\log N(\mathrm{H\ I}) = 18.5$–$20.0$ atom cm^{-2}. Nevertheless, the theory predicts little change in the form of the column density distribution function over the redshift range 2–4. This seems counter to current observations since a strong evolution of the number density of quasar absorbers with redshift has been derived (Péroux et al. 2002), implying a factor of 3 or more difference in the number of LLS between $z = 2$ and 4.

More importantly, the new set of observations can be directly compared with models of the column density distribution (Corbelli, Salpeter & Bandiera 2001; Zheng & Miralda-Escudé 2002). Zheng & Miralda-Escudé (2002), in particular, modelled DLAs as spherical isothermal gaseous haloes ionized by the external cosmic background to predict the column density distribution. Their models for different halo masses: 10^{12}, 10^{11}, 10^{10}, 10^9 M$_\odot$ (from top to bottom) are overplotted in Fig. 1. The normalization of the curves is arbitrary since it depends, among other things, on the size distribution of the clouds, which is not known, but the shape can be directly compared with the data. In addition, Zheng & Miralda-Escudé show that the column density at which the flattening takes place depends only on the neutral fraction in the absorber at the radius where self-shielding occurs. The present data exclude the models with high-mass haloes.

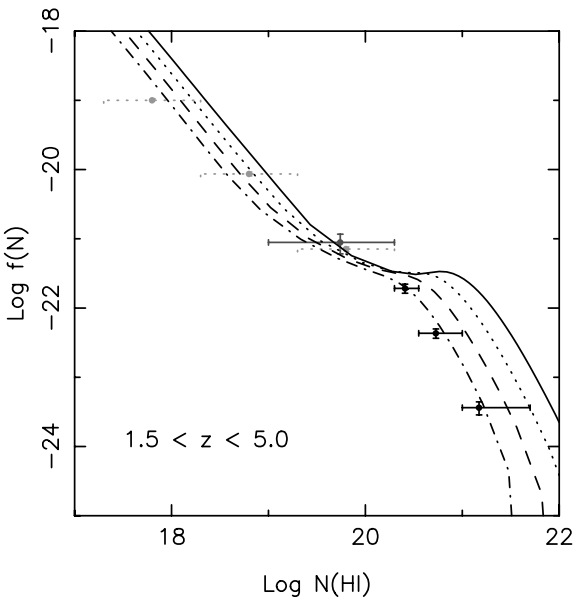

Figure 1. The solid bins at $\log N(\mathrm{H\ I}) > 20.3$ atom cm^{-2} are measurements of the column density distribution of DLAs from Péroux et al. (2002). The dashed bins [$17.2 < \log N(\mathrm{H\ I}) < 20.3$ atom cm^{-2}] are deduced from the fit to the observed cumulative number of quasar absorbers (Péroux et al. 2003), while the solid bin in the range $19.0 < \log N(\mathrm{H\ I}) < 20.3$ atom cm^{-2} is the observed number density of sub-DLAs from the UVES archive quasar spectra presented in this paper. Models (corrected to $\Omega_M = 0.3$, $\Omega_\Lambda = 0.7$ cosmology) of Zheng & Miralda-Escudé (2002) with halo masses of 10^{12}, 10^{11}, 10^{10}, 10^9 M$_\odot$ (from top to bottom) are overplotted. The vertical normalization of the curves is unconstrained in the models and thus on this figure the lines are arbitrarily shifted to best fit the data points. On the other hand, the shape of the model distributions can be directly compared with the data in order to determine the neutral fraction in the absorber at the radius where self-shielding starts to be important (see the text for further explanation).

Moreover, according to Péroux et al. (2002), the change of slope of the column density distribution should evolve with redshift, moving out in redshift from $z = 2$ to 4. Unfortunately, the current sub-DLA sample is not sufficient to study the evolution with redshift of the distribution down to $N(\mathrm{H\ I}) = 10^{19}$ atom cm^{-2}. More data are required at high redshift in order to be able to probe the evolution with time of the properties of the sub-DLAs.

3 CLUSTERING OF SUB-DLAS

As already noted all the quasars studied here were extracted from the ESO UVES archive and so the large majority were observed because there was a DLA along their line of sight. Although the DLAs themselves were excluded from the redshift path surveyed in the quasar, it is of interest to note that on at least one occasion, the sub-DLA discovered is situated in the wing of a known DLA: $z_{\mathrm{sub\text{-}DLA}} = 2.557$ and $z_{\mathrm{sub\text{-}DLA}} = 2.466$ towards Q1223+1753, giving

$dz = 0.09$, corresponding to $\Delta v \sim 8000$ km s^{-1} (see Paper I). In addition, we note that out of the 12 sub-DLAs that make up our sample, at least three systems ($z_{\rm sub\text{-}DLA} = 1.996$ towards Q2116−358, $z_{\rm sub\text{-}DLA} = 3.565$ towards PSS J2155+1358 and $z_{\rm sub\text{-}DLA} = 3.882$ towards PSS J2344+0342) cannot be fitted with only one absorption system, suggesting the presence of smaller column density absorbers in their close vicinity (see Paper I for more details on these systems). Obviously, these features illustrate the difficulty in determining the H I column density of sub-DLA systems and differentiating these objects from a conglomerate of smaller column density objects. In the particular cases of $z_{\rm sub\text{-}DLA} = 3.356$, 3.589 and 4.214 towards BR J0307−4945, we cannot estimate the size and the number of absorbers involved. We refer the reader to Section 3.1 of Paper I for a discussion of these specific cases.

To summarize, our sample of 12 sub-DLAs contains four systems associated with other absorbers, one of which is a DLA, the remaining being smaller column density systems. From Péroux et al. (2002), the expected probability of absorbers with $N({\rm H}) > 10^{19.0}$ atom cm^{-2} is $n(z) \sim 0.4$ at $z \sim 2.5$, if the absorbers were randomly distributed. Thus there is only a 1 in 50 chance of finding quasar absorbers separated by $dz = 0.09$ ($\Delta v \sim 8000$ km s^{-1}). The observed incidence of clustered absorbers (1 out of 12) is therefore higher than expected. For comparison, out of the hundreds of DLAs known today, only three cases of such clustering along a given line of sight have been reported in the literature. Prochaska & Wolfe (1999) report a pair of DLAs towards Q2359−02 at $z = 2.1$ and separated by $\Delta v \sim 5700$ km s^{-1}. Ellison & Lopez (2001) have presented a pair of (strictly speaking) DLA/sub-DLA at $z = 1.8$ separated by $\Delta v \sim 2000$ km s^{-1}, which are characterized by a low-α/Fe elemental ratio. Lopez et al. (2001) have found three DLAs at $z = 2.6$ in CTQ 247 separated by $\Delta v \sim 6000$ km s^{-1}, which show similar abundance patterns (Lopez & Ellison 2003).

The quantitative interpretation of this phenomenon is not straightforward. Lyman-break-selected galaxies (e.g. Steidel, Adelberg & Dickinson 1998) and Lyα-emitting galaxies (Ellison et al. 2001) have been shown to be clustered at high redshifts. Similarly, studies of transverse clustering from quasars pairs or groups show a highly significant overdensity of strong absorption systems over separation lengths from ∼1 to $8h^{-1}$ Mpc (D'Odorico, Petitjean & Cristiani 2002). Our findings are therefore not surprising in that respect. In all cases, pairs of sub-DLAs/DLAs are potentially of great interest since, in such cases, one could reasonably assume that the incident radiation field is similar for both absorbers, thus providing further information on the otherwise poorly constrained photoionization spectrum. Such studies would nevertheless require a good estimate of H I column density of each system (often requiring other lines down the Lyman series) and that the metals associated with each absorber are well characterized.

4 KINEMATICS OF SUB-DLAS

The kinematic properties of quasar absorbers can be used to provide further information on their nature. Using various line diagnostics to parametrize the symmetry, velocity width and the edge-leading profiles of the metal lines of 17 DLA systems, Prochaska & Wolfe (1998) suggest that the absorbers are fully formed, large, rapidly rotating galactic discs with $v_{\rm circ} \gtrsim 200$ km s^{-1}. More recently, Wolfe & Prochaska (2000b) have used a sample of 35 DLAs (Wolfe & Prochaska 2000a) and compared them with semi-analytical models of galaxy formation. They note that none of the models reproduce the overlap between low- and high-ionization metal profiles observed in the data. In addition, this scenario is in stark contrast with the currently favoured hierarchical structure formation models, where present-day galaxies are assembled from virialized subunits over a large redshift range ($z \sim 1$–5). Other hydrodynamic N-body simulations and semi-analytical models (Haehnelt, Steinmetz & Rauch 1998; Maller et al. 2001, 2002) have shown that the low ion absorption profiles can equally well be interpreted as a signature from merging protogalactic clumps in collapsing dark matter *haloes* with small virial velocities (∼100 km s^{-1}). In addition, Ledoux et al. (1998) have used a sample of 26 DLAs and find a correlation between the asymmetry and ΔV for $\Delta V \lesssim 150$ km s^{-1}. They suggest that this correlation is evidence that rotation velocities may dominate the narrower metal lines.

4.1 Sub-DLAs characteristics

First we examine the number of components necessary to fit the low-ionization transitions of the sub-DLAs, noting that out of 12 systems, five require more than 10 components. We also note that most of the remaining systems (another five absorbers) are well fitted with only three or fewer components.

We chose to describe the properties of the lines of the low- and high-ionization transitions in our sample of sub-DLAs with the help of four simple quantities, namely:

(i) $\Delta_{\rm low}$, the width of the low-ionization transitions as measured from the most saturated Fe II or Si II lines;

(ii) $\Delta_{\rm high}$, the width of the high-ionization transitions as measured from the most saturated C IV or Si IV lines;

(iii) δv, the offset between the mean velocity of the high- and low-ionization transitions;

(iv) $f_{\rm ratio}$, the ratio of the velocity widths of the high- and low-ionization transitions.

All of these parameters are used to quantify the differences between various states of the gas observed in absorption. The shift between the low- and high-ionization transitions for our sample of sub-DLAs is shown in Fig. 2 for the eight systems where high-ionization transitions are detected. In most cases, although the two sets of absorption overlap, the profiles are widely different. In one particular object ($z_{\rm abs} = 3.171$ in Q1451+123), Si II is not superimposed at all on the C IV doublet in velocity space, the two being separated by ∼75 km s^{-1}. It might be that the C IV doublet is actually not associated with the sub-DLA itself (see Paper I for more details). As in DLAs, the high-ionization transitions spread over larger velocity intervals than their low-ionization counterparts, but their correspondence suggests that the systems are within the same potential well (Wolfe & Prochaska 2000b). However, in two cases ($z_{\rm abs} = 3.882$ in Q2344+034 and $z_{\rm abs} = 2.087$ in Q1444+014), the low-ionization transitions traced by Si II spread over a larger velocity interval than the high-ionization transitions.

4.2 Comparison with DLAs

In order to compare the kinematic properties of sub-DLAs with DLAs, we have determined the parameters described in the previous section for 72 DLAs taken from the literature. The systems quoted are from a mixture of UVES/HIRES and lower-resolution spectrographs for high-redshift targets, and from the *Hubble Space Telescope* at lower redshifts. 13 additional sub-DLAs are found in the literature. We made the relevant measurements from the quasar spectra whenever we had them, otherwise we directly used the original publications to quantify the width of the ion lines. We

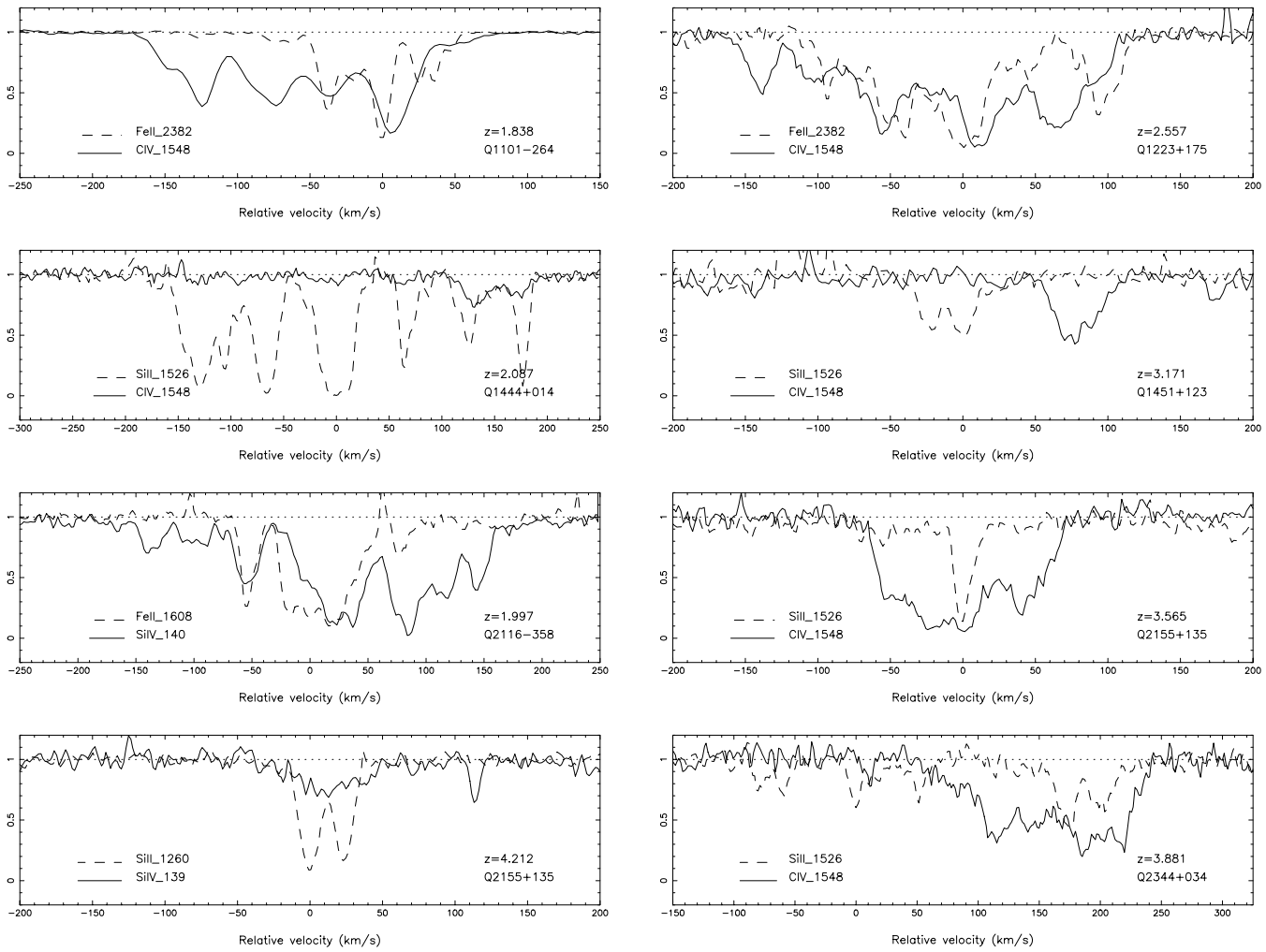

Figure 2. Velocity space superposition of the low- (Fe II or Si II) and high-ionization (C IV or Si IV) transition profiles for the sub-DLAs of our sample where high-ionization transitions are detected. The two states of the gas overlap in most cases apart from $z_{\rm abs} = 3.171$ in Q1451+123. This figure is available in colour in the online version of the journal on *Synergy*.

preferentially used the Fe II and C IV lines whenever possible. In addition, if the data came from the UCSD HIRES/KeckI survey (Prochaska & Wolfe 1998, 2000, 2002; Prochaska, Gawiser & Wolfe 2001; Prochaska et al. 2002), we took the velocities used for the optical depth method given on the web page of the survey[1] kindly provided to the general community and maintained by Jason X. Prochaska.

The resulting distributions for $\Delta_{\rm low}$, $\Delta_{\rm high}$, δv and $f_{\rm ratio}$ are illustrated in Fig. 3. Although the number of sub-DLAs is still small, it appears that their velocity spreads in both low- and high-ionization transitions are statistically equivalent to the DLAs (top left and top right-hand panel of Fig. 3). In most cases, the shift between the low- and high-ionization transitions is small in DLAs (less than 20 km s^{-1}) (bottom left-hand panel of Fig. 3). Finally, the $f_{\rm ratio}$ values of DLAs and sub-DLAs are comparable (bottom right-hand panel of Fig. 3). These measurements are important to constrain semi-analytical models. Indeed, Maller et al. (2002) find that a large fraction of absorbers with $\log N({\rm H\,I}) > 20.0$ cm^{-2} might be composed of multiple component discs. In contrast, they predict that the smaller systems [in particular, those with $4 \times 10^{19} < N({\rm H\,I}) < 10^{20}$ cm^{-2}] will mostly be single discs. Therefore, δv is expected to be smaller in these systems than in classical DLAs. Although our data set is still small, the observations presented here do not support this interpretation, thus challenging multiple-component models. A possible explanation is that some of the low-ionization gas in sub-DLAs is in hot gas. Indeed, the data show a hint of decreasing $f_{\rm ratio}$ with lower column densities, therefore suggesting that the high and low ions are in the same gas at lower N(H I).

5 CHEMICAL ABUNDANCES OF SUB-DLAS

5.1 Ionization fraction

In Paper I, we have presented the hydrogen and ionic column densities of all of the sub-DLAs included in Table 1, using standard Voigt profile fitting. Since their relatively low column density implies that some of the gas might be ionized, the ionization state of the sub-DLAs has been investigated in detail in Paper I using the photoionization models of the CLOUDY software package. The determination of the ionization parameter U for a given absorber system crucially depends on the detection of intermediate-ionization

[1] http://kingpin.ucsd.edu/∼hiresdla/

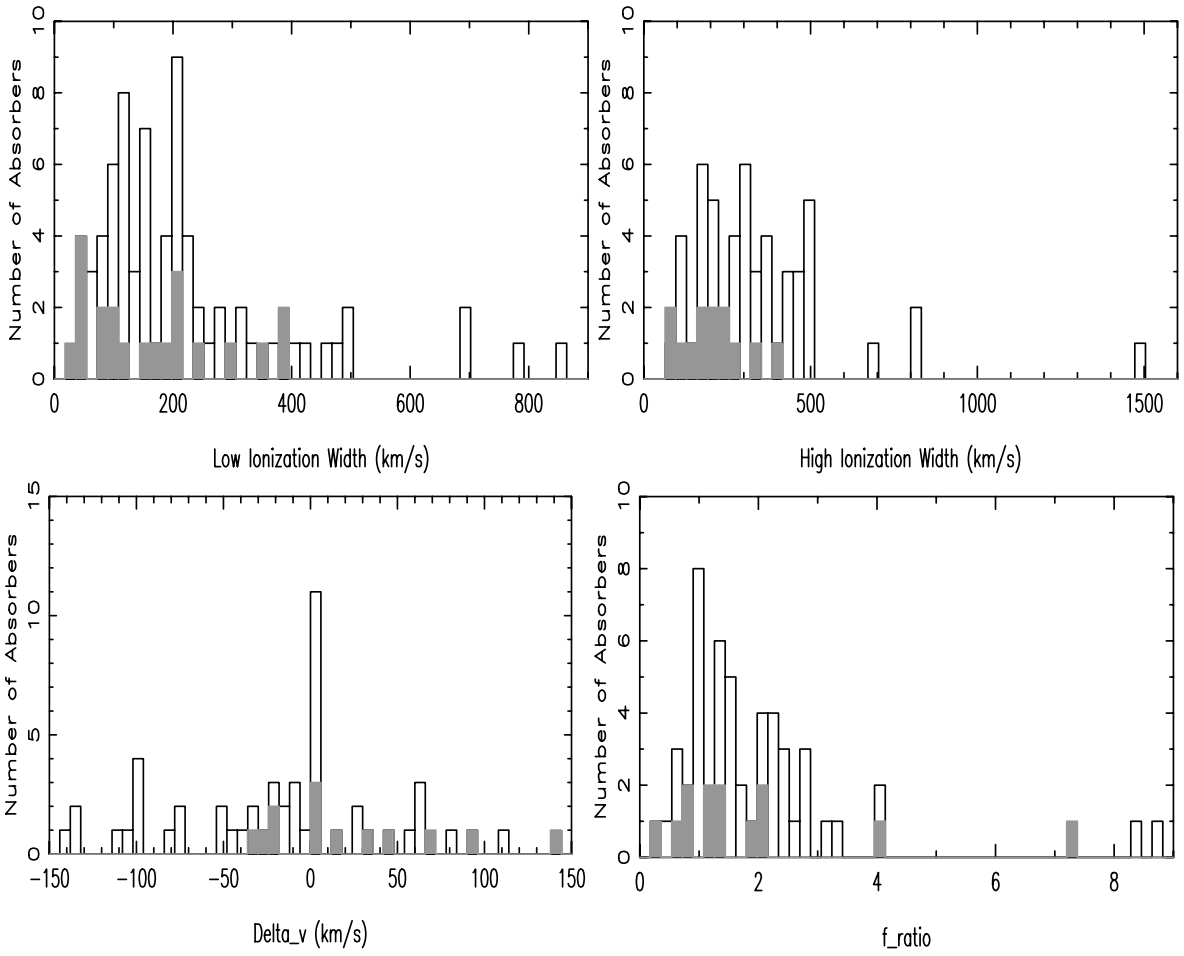

Figure 3. Comparison of the kinematic properties of DLAs (black line) and sub-DLAs issued from both our sample and the literature (light coloured histogram). The parameters plotted are (from left to right, from top to bottom) $\Delta_{\rm low}$, $\Delta_{\rm high}$, δv and $f_{\rm ratio}$. Although the statistics on sub-DLAs are still small it seems that their properties roughly span the parameter space of the DLAs, thus challenging multicomponent semi-analytical models. This figure is available in colour in the online version of the journal on *Synergy*.

transitions. In addition, the photoionization model relies on several input parameters related to the nature of the absorber and the characteristics of the radiation field. In this context we chose to extract from our analysis a global ionization correction rather than individual corrections limited by partial information. We found the correction to be < 0.3 dex for most elements down to N(H I) = 19.3 cm^{-2}. We also note that the correction to apply is quite different from one species to another. In the case of O I or C II, for example, the ionization fraction is small, while it becomes important for such elements as Al II or Zn II. One needs to keep these facts in mind while interpreting the various figures presented in the following sections.

5.2 Metallicity evolution

In this section, we present the results of the metallicity study of the sample of sub-DLAs and compare them with the characteristics of the well-studied DLAs. The references for absorbers from the literature are the same as in Section 4.2. The chemical abundances in DLAs have been used to trace the metallicity evolution of galaxies over a large look-back time (e.g. Pettini et al. 1999; Prochaska & Wolfe 2000) and contrary to virtually all chemical models, the observations in DLAs indicate mild evolution with redshift. By extending the abundance determination to systems of lower column densities, such as the sub-DLAs, we can gain insight into the evolution of the galactic chemical evolution of galaxies, since they are more likely to represent the basic building blocks of hierarchical growth of structure.

5.2.1 Metallicity of individual systems

[Fe/H]. Given that the ionization correction on the Fe II column density is within the observational errors, the abundance measurements of the sub-DLAs can be directly compared with those of the DLAs gathered from various sources in the literature. We use the abundance ratios with respect to solar values defined in the usual manner[2] and presented in Paper I. For the sake of homogeneity we recompute these ratios for all data from the literature assuming [Fe/H]$_\odot = -4.50$ (Grevesse & Sauval 1998). The top panel of Fig. 4 presents the evolution with redshift of the [Fe/H] absolute abundances in individual systems. The symbol sizes in this figure are proportional to the H I column density of the systems.

[2] [X/H] = $\log[N(\rm X)/N(\rm H)]_{\rm DLA} - \log[N(\rm X)/N(\rm H)]_\odot$, assuming that N(X) = N (*X ii*) and N(H) = N(H I).

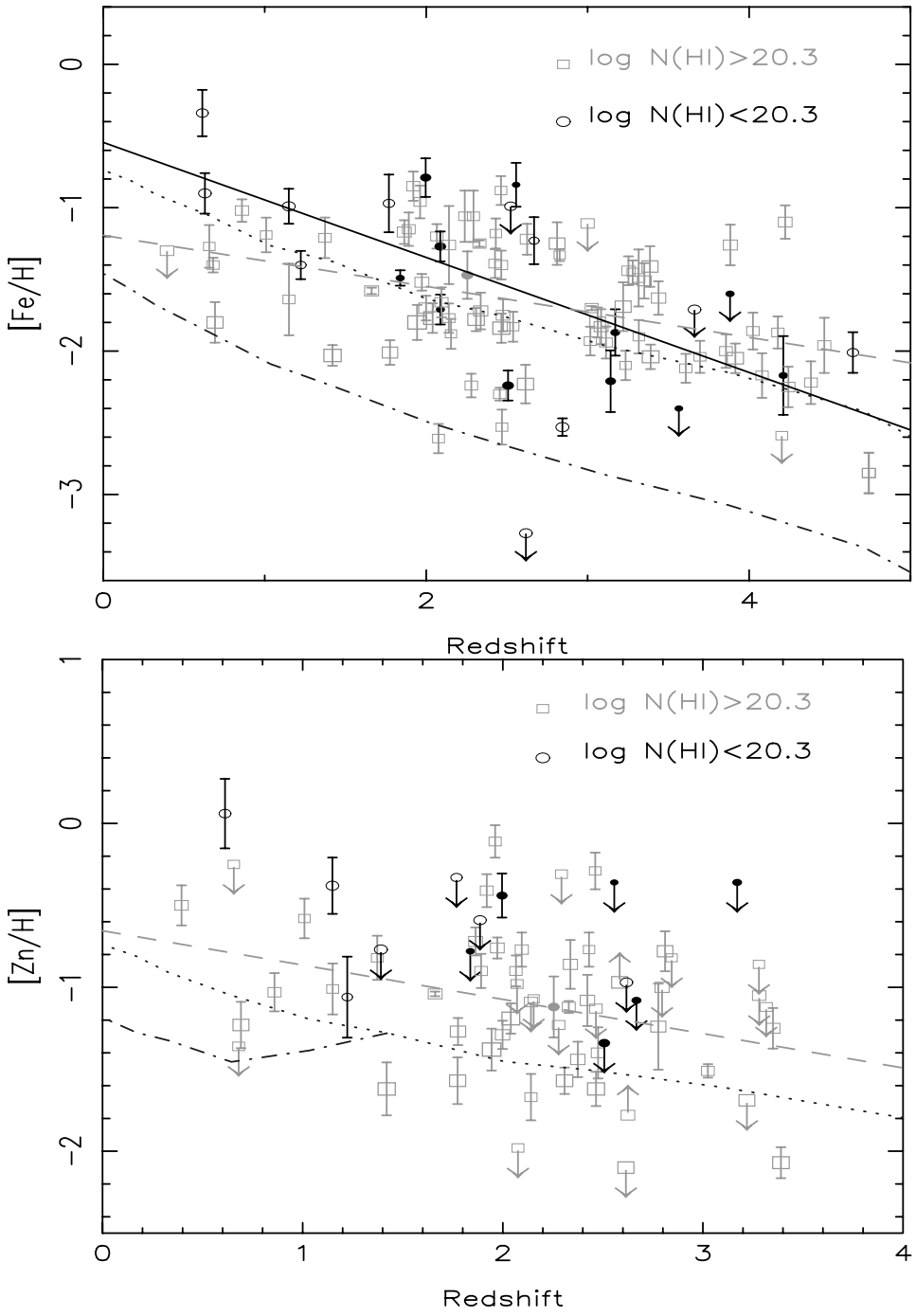

Figure 4. [Fe-Zn/H] metallicities for DLAs (squares) and sub-DLAs (open circles for data from the literature, filled circles for the sub-DLAs from this work) as a function of redshift. The symbol sizes are proportional to the H I column density of the systems. The evolution with redshift of the [Fe/H] ratio is more pronounced for sub-DLAs than for DLAs (solid and dashed lines, respectively). The dashed-dotted (dotted) curves are results from models from Hou et al. (2001) for sub-DLAs (DLAs). This figure is available in colour in the online version of the journal on *Synergy*.

The classical DLAs are represented with square symbols while the sub-DLAs are circles (open for data from the literature, filled for the data from the sample presented in this paper). We applied the order ranking Kendall test to several subsets of the sample as shown in Table 3, ignoring all upper and lower limits. As previously reported (e.g. Dessauges-Zavadsky et al. 2001; Prochaska & Wolfe 2002), there is evidence for a mild evolution of the individual [Fe/H] in DLAs (correlation coefficient of -0.29 at 99.53 per cent confidence level). The analysis suggests a stronger correlation of the [Fe/H] in sub-DLAs, although the significance of the test is weakened by low number statistics (correlation coefficient of -0.50 at 84.27 per cent confidence level for a total of 17 sub-DLAs). The effect is predominant at $z < 2$ and most of the evolution observed lies in this redshift range. We fitted the two populations of absorbers assuming a linear correlation and found a slope of $\alpha = -0.18 \pm 0.12$ for DLAs and $\alpha = -0.40 \pm 0.22$ for sub-DLAs (dashed and solid line

Table 3. Results from the order ranking Kendall test and slopes of the fits assuming a linear correlation for different subsets of quasar absorbers, ignoring all upper and lower limits. The lack of correlation between the redshift and [Fe/H] is due to the larger column density systems (log N(H I) > 21.0). In contrast the sub-DLAs appear to show more correlation, with a more pronounced slope, although the results are still weakened by low number statistics.

Data set definition	No of abs	τ	CL	Slope
log N(H I) $\geqslant$ 20.3	72	−0.29	99.53 per cent	-0.18 ± 0.12
log N(H I) < 20.3	17	−0.50	84.27 per cent	-0.40 ± 0.22
log N(H I) < 21.0	75	−0.40	99.99 per cent	-0.28 ± 0.11
All absorbers	89	−0.35	99.53 per cent	-0.24 ± 0.11

of the top panel of Fig. 4, respectively). The evolution with redshift of the [Fe/H] ratio might be more pronounced for sub-DLAs than for DLAs. This difference, if confirmed by a larger sample of data, suggests that the detection of DLAs is more biased by dust at low redshift, or that the sub-DLAs are associated with a class of galaxies that better trace the overall chemical evolution of the Universe.

[Zn/H]. The well-known drawback of using Fe II for abundance determination is the fact that this element is sensitive to depletion on to dust grains (Pettini et al. 1997). An alternative to overcome the dust depletion issue is provided by Zn, an element known to be only mildly depleted. The lower panel of Fig. 4 presents the evolution of the [Zn/H] with redshift. Again for the sake of homogeneity we recompute these ratios for all data from the literature assuming $[\mathrm{Zn/H}]_{\odot} = -7.33$ (Grevesse & Sauval 1998). In our sample of sub-DLAs, most of the Zn II lines are weak or undetected and thus we can only provide upper limits. In addition, the ionization correction in sub-DLAs is important for Zn II and thus the interpretation of the abundances is more complicated. We again used the order ranking Kendall test for the subsets of the Zn II sample. When considering both DLAs and sub-DLAs (and excluding all limits), we determine a slope of $\alpha = -0.28 \pm 0.23$, i.e. slightly shallower than that derived by Vladilo et al. (2000) and Dessauges-Zavadsky et al. (2001) ($\alpha \sim -0.3$) since the latter works loosely include sub-DLAs in their samples. Nevertheless, the significance of this result is low (correlation coefficient of −0.25 at 84.27 per cent confidence level for a total of 40 abundances). Analysing DLAs only, leads to a slope $\alpha = -0.21 \pm 0.25$ for 36 systems. There are not enough Zn II measurements in the sub-DLAs range to allow such an analysis. An important point, however, is the fact that the slope in the Zn II DLA subset ($\alpha = -0.21 \pm 0.25$), a tracer of true metallicity evolution, is not as steep as in the Fe II sub-DLA subset ($\alpha = -0.40 \pm 0.22$). This suggests that the evolution we probe in these latter absorbers is *not* due to the hidden effect of dust.

Comparison with models. These observational results can be compared with models of galaxy evolution and the corresponding evolution of metal abundances to further test the nature of quasar absorbers. Complications arise from the fact that the observed systems might have different formation epochs, a parameter that cannot be directly constrained by the data. Prantzos & Boissier (2000) use models of the chemical evolution of disc galaxies, calibrated on the Milky Way (Boissier & Prantzos 1999, 2000), which they then compare with the Zn abundances of DLAs. This comparison is extended to other elements in Hou, Boissier & Prantzos (2001). They find that the results are compatible with available observations, provided that several biases are taken into account, one of these biases being reproduced by applying a 'dust filter' to the models. This filter was proposed by Boissé et al. (1998), who suggest that high column density and high-metallicity systems are not detected because the light of background quasars is severely extinguished. This claim arises from the observed trend in [X/H] versus log N(H I) in quasar absorbers (see Section 5.2.3 for more on this issue). The results of the models are further constrained by the H I column density detection limits in current surveys. In Hou et al. (2001), this limit corresponds to the formal definition of DLAs, log N(H I) > 20.3. The mean [Fe/H] value of the model is presented in Fig. 4 as a dotted curve. The scatter in the observations is genuine (since it is higher than the error bars on individual metallicity measurements) and is well reproduced by the model (see fig. 2 of Hou et al. 2001).

Adjusting the threshold to the sub-DLA definition results in the dashed-dotted curve presented in Fig. 4. The models do not indicate a change in evolution with redshift between DLA and sub-DLA systems (see dotted and dashed-dotted curves in the bottom panel of Fig. 4). Rather they suggest that the metallicity in sub-DLAs is lower than in DLAs. This is a natural consequence of the abundance gradients observed in nearby galaxies and in the Milky Way, well reproduced by the models (Prantzos & Boissier 2000). In contrast, the observations indicate that the sub-DLAs seem more metal-rich than the DLAs, at least at low redshift. Therefore, although the disc models are in quite good accordance with the DLA observations, the mismatch between these models and the sub-DLA observations suggests that sub-DLAs do not arise in disc galaxies.

The [Zn/H] observed redshift evolution can also be compared with models of galaxy evolution proposed by Hou et al. (2001). It should be emphasized that in the models, the Zn II abundance is set to follow the Fe abundance. The difference between the two arises only from different 'biases'; the current Zn detection can be accounted for by applying to the models the filter log N(H I) + [Zn/H] > 18.8, an estimate of the Zn limit detection (e.g. Prantzos & Boissier 2000). Again, setting the column density cut-off in the models to the DLA definition reproduces the trend well (dotted curve in the bottom panel of Fig. 4) and the scatter between measurements (see also Prantzos & Boissier 2000). Once the cut-off is chosen to match the sub-DLA definition (dashed-dotted curve in bottom panel of Fig. 4), the models suggest that the Zn II abundances in the systems at redshift greater than ∼1.3 are below current detection limits. This is indeed what is observed since most of the [Zn/H] presented here are upper limits. Note that to be able to measure the Zn abundance [log N(H I) + [Zn/H] > 18.8] in sub-DLAs, the system must satisfy [Zn/H] > −1.5.

Alternative modelling approaches have been recently proposed using hydrodynamic simulations to reproduce the gas and metal evolution observed in DLAs (Cen et al. 2003; Nagamine et al. 2003a,b). They find that the slow metallicity evolution currently observed in DLAs can be explained by the sequential formation of galaxies from the highest metallicity systems. This effect would be combined with increasing metallicity of the absorbers with the smallest abundances. Including an artificial cut-off in order to mimic the presence of dust in DLAs, the simulations are found to be in excellent agreement with the observations.

5.2.2 Weighted mean metallicity

Since DLAs and sub-DLAs are known to contain a major fraction of the neutral gas at all redshifts (Péroux et al. 2003), all of these systems should be used to probe the metallicity of the Universe

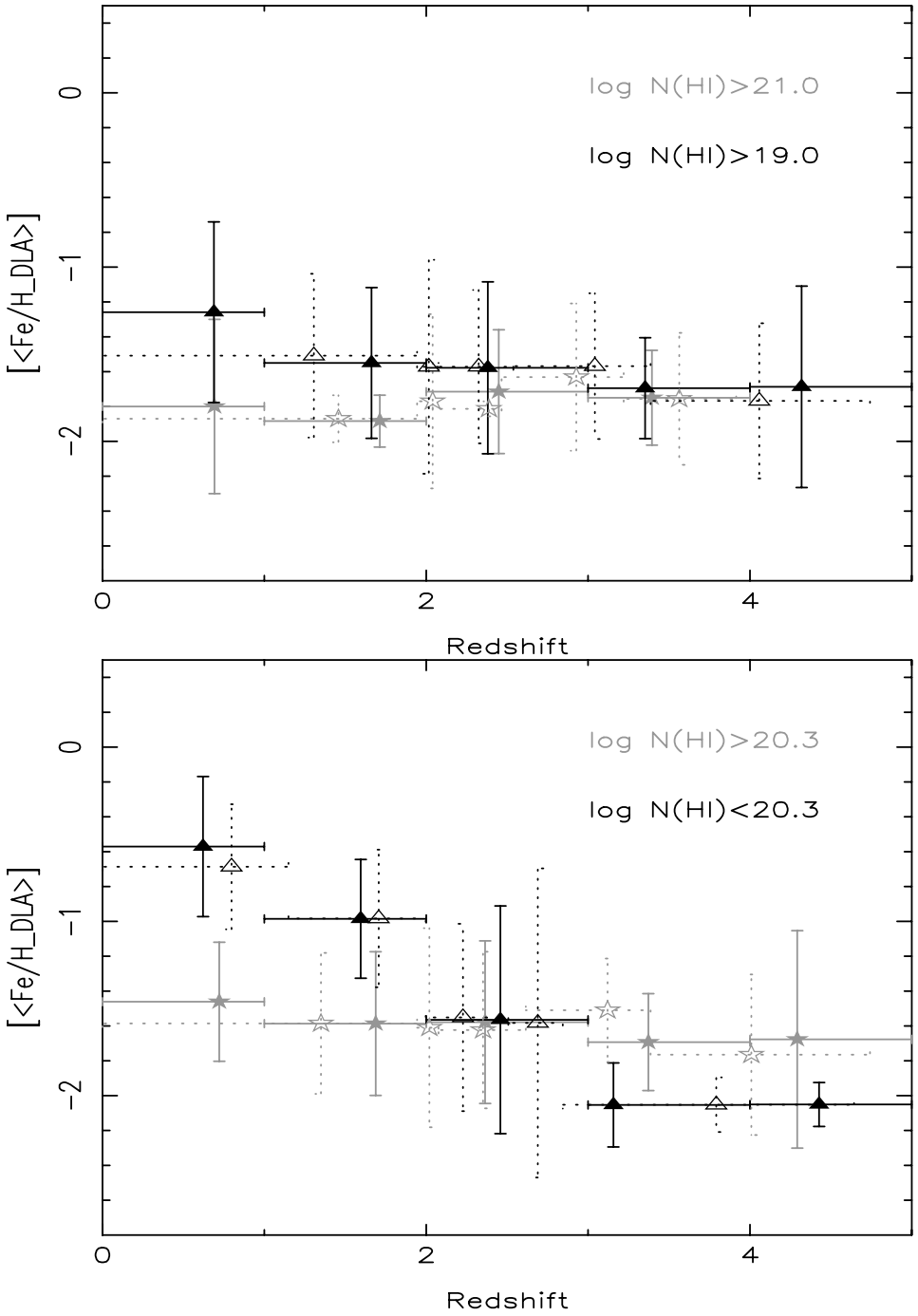

Figure 5. H I column-density-weighted mean metallicities for various subsets of quasar absorbers. The dotted bins are for constant H I intervals and the solid bins are for constant redshift intervals. The evolution of $[\langle \mathrm{Fe/H_{DLA}} \rangle]$ is clearly more pronounced for sub-DLAs than for DLAs, but this result is not apparent when all absorbers with $N(\mathrm{H\,I}) > 10^{19.0}$ atom cm^{-2} are considered. Indeed, in our sample the number of DLAs (72) is much larger than the number of sub-DLAs (17). This figure is available in colour in the online version of the journal on *Synergy*.

and its evolution with time. A quantitative way of estimating this evolution is provided by the H I-weighted mean metallicity. Pettini et al. (1997) state that 'under the working assumption that DLAs account for most of the material available for star formation at high redshift, the quantity $[\langle \mathrm{X/H_{DLA}} \rangle]$ (X = Fe or Zn) is a measure of the degree of metal enrichment by the Universe at a given epoch'.

Fig. 5 presents the column-density-weighted mean Fe II abundances of n systems in redshift bins of $\Delta z = 1$ (solid bins) and in constant H I interval (dashed bins), for various subsamples of quasar absorbers. Although more advanced statistical methods have been recently suggested (Kulkarni & Fall 2002), we choose to follow the prescription from Pettini et al. (1997):

$$[\langle \mathrm{Fe/H_{DLA}} \rangle] = \log\langle (\mathrm{Fe/H})_{\mathrm{DLA}} \rangle - \log(\mathrm{Fe/H})_{\odot}, \quad (3)$$

where

$$\langle (\mathrm{Fe/H})_{\mathrm{DLA}} \rangle = \frac{\sum_{i=1}^{n} N(\mathrm{Fe\,II})_i}{\sum_{i=1}^{n} N(\mathrm{H_{total}})_i} \quad (4)$$

and the errors are estimated from the standard deviation, σ':

$$\sigma'^2 = \left\{ \sum_{i=1}^{n} ([\mathrm{Fe/H}]_i - [\langle \mathrm{Fe/H_{DLA}} \rangle])^2 \right\} \Big/ (n-1) \quad (5)$$

with

$$[\mathrm{Fe/H}]_i = \log(\mathrm{Fe/H})_i - \log(\mathrm{Fe/H})_\odot. \quad (6)$$

The results of these calculations are shown in Fig. 5 for different subsets of quasar absorbers. The top panel includes all quasar absorbers (DLAs + sub-DLAs) and systems with $N(\mathrm{H\,I}) > 10^{21.0}$ atom cm^{-2}. The bottom panel shows DLA and sub-DLAs separately. We note that the evolution of $[\langle \mathrm{Fe/H_{DLA}} \rangle]$ is clearly more pronounced for sub-DLAs than for DLAs, but this result is not apparent when all absorbers with $N(\mathrm{H\,I}) > 10^{19.0}$ atom cm^{-2} are considered. Indeed, in our sample the number of DLAs (72) is much larger than the number of sub-DLAs (17). In contrast, in the Universe we expect the number of sub-DLAs to be up to three times (at $z \sim 4$) the number of DLAs (Péroux et al. 2002). Since high column density systems dominate the HI-weighted mean metallicity, it will be important to increase the sub-DLA sample size to better probe $[\langle \mathrm{Fe/H_{DLA}} \rangle]$. Nevertheless, these results show that the H I column-density-weighted mean metallicity Fe II of sub-DLAs *do* evolve with redshift more markedly than for the DLA population. The dotted bins correspond to constant H I intervals and therefore present a similar number of systems. They also reveal an increase of metallicity with decreasing redshift, showing that this result is not an artefact of the low number of sub-DLAs known at $z < 2$. Starting from a metallicity of $1/100$ solar at $z \sim 4.5$, the sub-DLAs evolve up to a metallicity of $1/3$ solar at $z \sim 0.5$. The ionization correction cannot explain the evolution observed since we have shown in Paper I that for [Fe II/H I], it *does not* exceed 0.2 dex. These results again reinforce the hypothesis that sub-DLAs better trace the global metallicity evolution and therefore should be included in the metallicity determination to obtain a complete picture of the abundance.

5.2.3 Correlating with other properties

[Fe-Zn/H] versus H I. Fig. 6 presents [Fe-Zn/H] as a function of H I column density for DLAs and sub-DLAs in three different redshift ranges: $z < 2$, $2 < z < 3$ and $z > 3$. In the top panel ([Fe/H]), the spread of values is larger at lower H I column densities. This suggests that we are sampling a different class of objects, or at least different parts of the same object as suggested by, for example, Boissier, Péroux & Pettini (2003). Another possibility is that dust plays an important role in the diversity of properties through a range of star formation histories. In contrast, there is little spread in the [Fe/H] ratio at very high H I column densities [$\log N(\mathrm{H\,I}) > 21$], posing the question of why these systems differ from the other quasar absorbers. This might indicate that systems with high column densities belong to a well-defined population of objects, though more probably, the lack of apparent spread could be the result of a bias against high column density, high metallicity absorbers due to their high dust content (Boissé et al. 1998). Indeed, the bottom panel of Fig. 6 shows that the observational bias noted by Boissé et al. in the H I versus [Zn/H] relation, still holds (i.e. no data are situated above the $[\mathrm{Zn/H}] + \log N(\mathrm{H\,I}) > 21$ solid line). A direct dust diagnostic in sub-DLAs is not straightforward to make since Zn II is seldom detected. Using the three Zn II detections in our sample of 12 systems, we find that the [Zn/Fe] value is around 0.3–0.4 dex. This suggests that the amount of dust is not negligible, although naturally there are too few detections to draw any firm conclusions. In addition, a study of absorbers derived from a radio-selected quasar sample (CORALS) does *not* indicate that a dust bias greatly affects DLA studies (Ellison et al. 2001), but in the authors' own words the conclusions are only tentative due to the limited size of the data set. Furthermore, in the range $20.0 < \log N(\mathrm{H\,I}) < 21.0$, i.e. the bulk of the data available, the high-redshift objects are less evolved than the others. In any case, we find that the metallicity evolution of quasar absorbers is a strong function of the H I column density. In addition, we have shown that the ionization correction in Fe II (see Paper I) is similar within a group of systems with similar column densities. In the sub-DLA range, it tends to increase the Fe II column density measured by 0.1–0.2, thus not affecting the apparent evolution.

[Fe-Zn/H] versus kinematic properties. Fig. 7 presents the metallicity of quasar absorbers as a function of their kinematic properties (Δ_{low}, Δ_{high}) as measured in Section 3. The symbol shapes denote different redshift ranges. The open symbols are for DLAs and the filled symbols are for sub-DLAs. The results indicate that in most cases the properties are homogeneously mixed between samples of different H I column densities or redshifts. The boxes represent the mean in a given velocity interval with rms errors and suggest an increase of metallicity towards larger ionization widths, although the statistical significance of this result is low.

5.3 Relative abundances

The comparison of elemental ratios, independent of H I column density, but as a function of metallicity is also very important. We concentrate in particular on the α (i.e. O, Si) over Fe-peak element ratios versus [Fe/H] metallicities, since this relation provides information on the star formation histories of quasar absorbers. $[\alpha/\mathrm{Fe}]$ versus [Fe/H] is a strong function of the star formation history: α/Fe depends on the lifetimes of the element progenitors, whereas [Fe/H] depends on the star formation rates. The α elements are typical products of type II supernovae, which are likely to dominate the early stages of galaxy formation. Fe-peak elements, in contrast, are products of type Ia supernovae, which play a role in later evolutionary stages. Therefore, high overabundances of α elements at low [Fe/H] indicate recent star formation, while solar α element abundances at low [Fe/H] suggests a lower star formation rate or bursts separated by quiescent periods. Nevertheless, the interpretation of these elemental ratios is once again complicated by differential depletion: Fe II and Si II are known to be depleted on to dust grains in different proportions while O I is expected to remain unaffected by dust depletion.

[Si/Fe]. Fig. 8 shows that [Si/Fe] is similar in both DLAs and sub-DLAs, averaging around +0.5 dex. For the sake of homogeneity we recompute these ratios for all data from the literature and models assuming $[\mathrm{Si/H}]_\odot = -4.44$ (Grevesse & Sauval 1998). This value is typical of Galactic metal-poor stars and is a strong indicator of α enhancement if dust depletion does not play a major role. Nevertheless, the differential depletion of these two elements can lead to the same enhancement as that observed. This observation can be directly compared with various models of galaxy formation and evolution. Models of Hou et al. (2001), with cut-off at the DLA and sub-DLA column density definitions, are presented in Fig. 8 as dark-coloured dashed and solid contours, respectively. In both cases, the models seem to underproduce the Si II abundance with respect to Fe in comparison with observations, but since the yields used in the

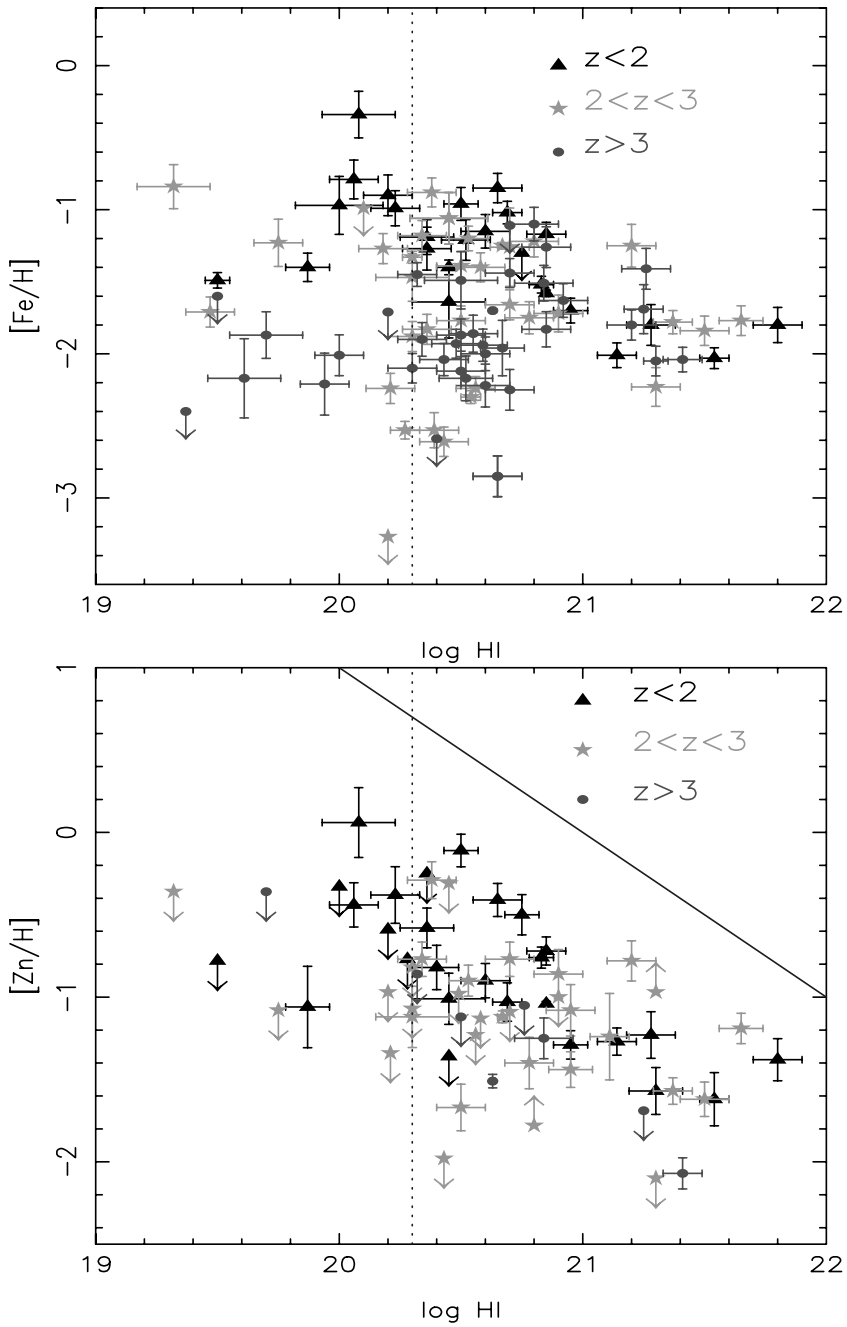

Figure 6. [Fe/H] and [Zn/H] as a function of H I column density in DLAs and sub-DLAs. The dotted line marks the DLA formal definition. On the bottom panel, the solid line corresponds to the 'dust filter' proposed by Boissé et al. (1998), namely [Zn/H] + log N(H I) > 21. This figure is available in colour in the online version of the journal on *Synergy*.

model are uncertain by a factor of 2, at best, it is unlikely that the absolute value of the abundance ratio is known with an uncertainty of better than 0.6 dex.

In an alternative approach, Calura, Matteucci & Vladilo (2003) have produced models for a variety of galaxy types. In Fig. 8, the light-coloured solid (dashed) curves are for spirals (irregulars). Indeed, in the chemical evolution models, irregulars are found to reproduce well the observed properties of DLAs. In these models, there is no artificial bias applied to mimic the effect of dust on the observations, nor was it necessary to add an extra H I column density cut-off to match the definition of the quasar absorbers. In the case of spiral galaxies, in particular, the models presented in Calura et al. (2003) never reach the sub-DLA column density since star formation is set to occur only above a density threshold, as suggested by Chiappini, Matteucci & Gratton (1997). In order to reproduce the properties of sub-DLAs, it has been necessary to eliminate this threshold and extend the computations towards larger radii (20 kpc). For [Si/Fe], the two types of models show little difference. In addition, the interpretation of this elemental ratio might be complicated by the effect of dust.

[O/Fe]. O I is not often measured in DLAs, since the most predominant line, O I 1302, is often saturated. In contrast, in sub-DLAs where the column densities are considerably smaller, this line is well suited

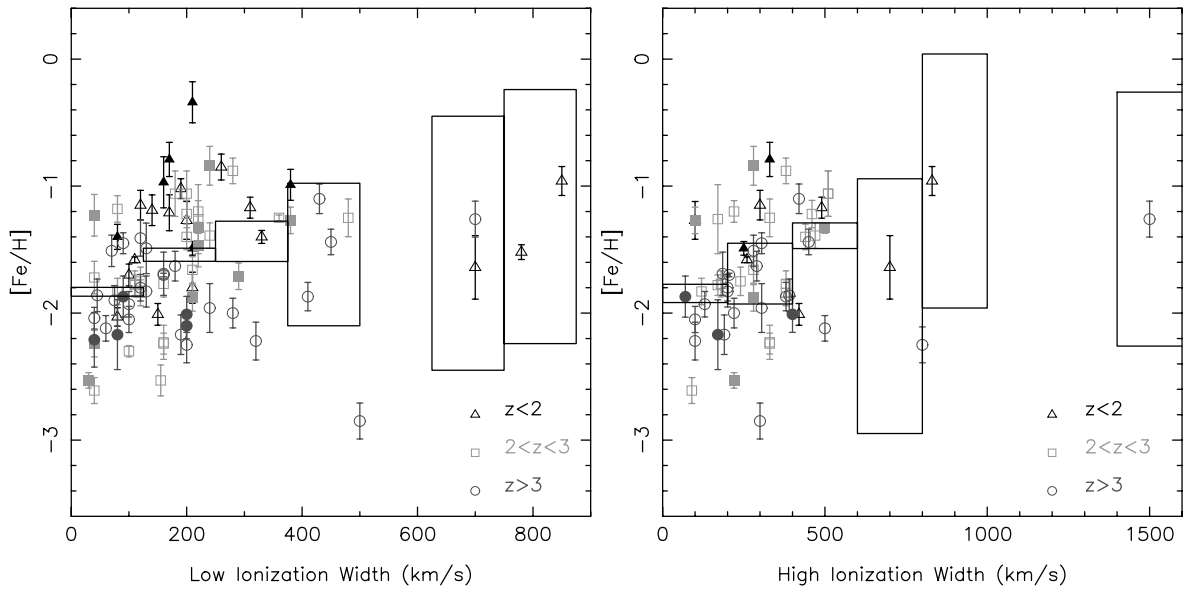

Figure 7. [Fe/H] as a function of various kinematic parameters: Δ_{low} and Δ_{high} (see Section 3 for details). The symbol shapes depict different redshift ranges. The open symbols are for DLAs and the filled symbols are for sub-DLAs. The boxes represent the mean in a given velocity interval with rms errors and suggest an increase of metallicity towards larger ionization widths. This figure is available in colour in the online version of the journal on *Synergy*.

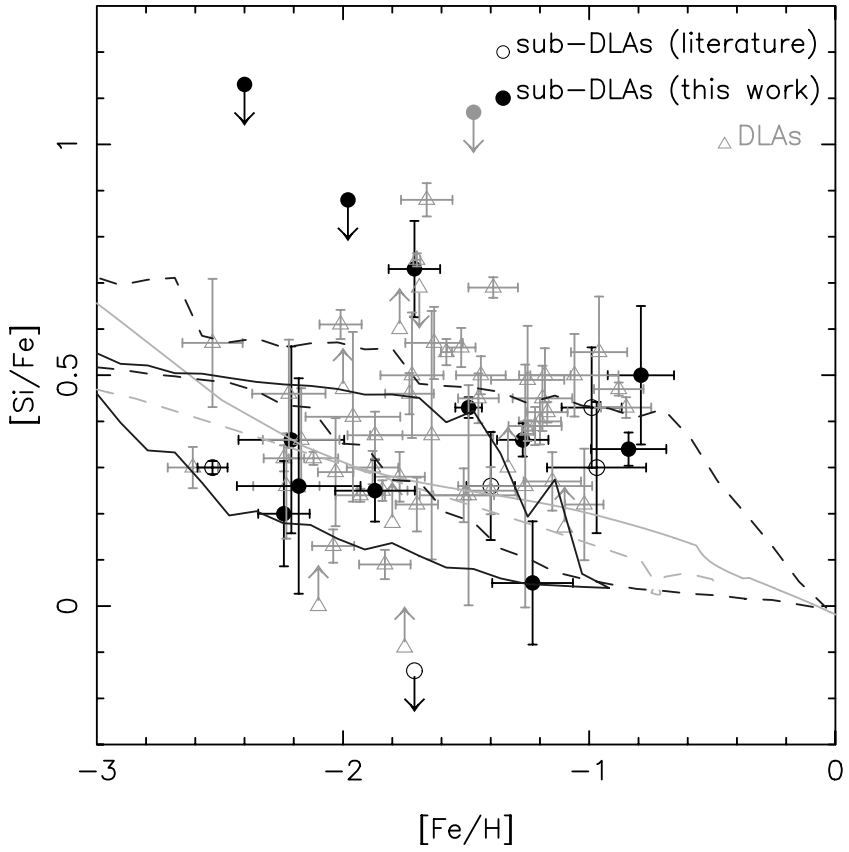

Figure 8. [Si/Fe] ratio as a function of metallicity. [Si/Fe] is similar in both DLAs and sub-DLAs. The dark-coloured solid (dashed) curves are contours for sub-DLAs (DLAs) column densities derived from models of disc galaxies (Hou et al. 2001). The light-coloured solid (dashed) curves are for spirals at 20 kpc (irregulars) representative of sub-DLAs (DLAs) in the models of (Calura, Matteucci & Vladilo 2003). This figure is available in colour in the online version of the journal on *Synergy*.

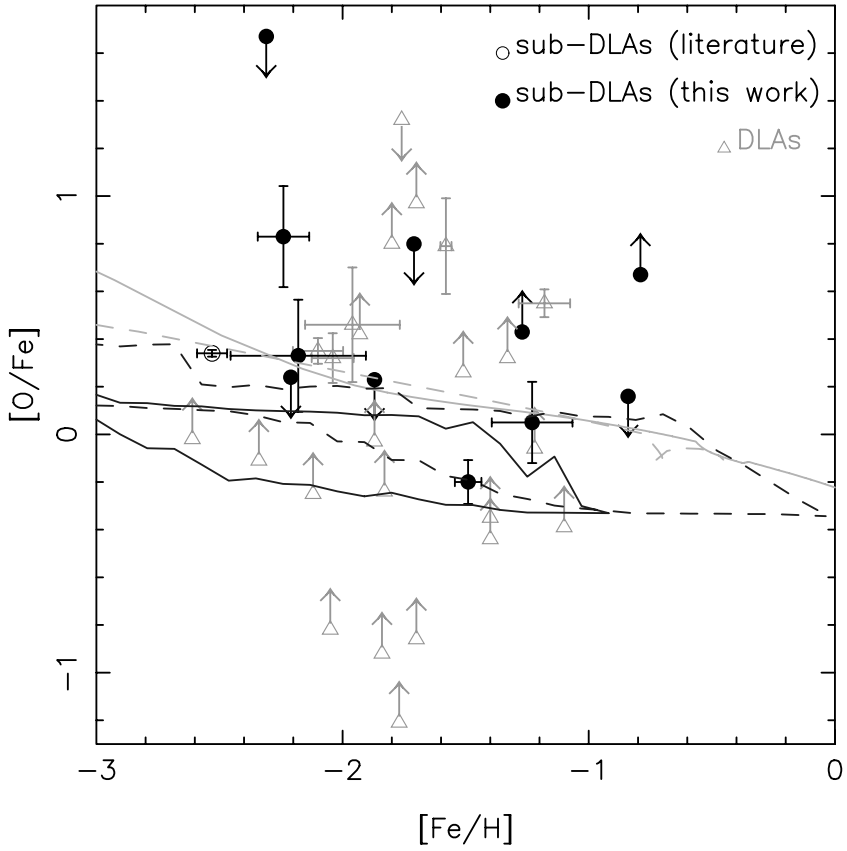

Figure 9. [O/Fe] ratio as a function of metallicity. At low metallicity the ratio are greater than solar. Sub-DLAs generally have low [O/Fe], some of which are subsolar. The dark-coloured solid (dashed) curves are contours for sub-DLAs (DLAs) column densities derived from models of disc galaxies (Hou et al. 2001). The light-coloured solid (dashed) curves are for spirals (irregulars) representative of sub-DLAs (DLAs) in the models of (Calura et al. 2003). This figure is available in colour in the online version of the journal on *Synergy*.

for the abundance determination of oxygen. This element, which is not affected by dust depletion, is also a typical product of type II supernovae. The prospect of measuring O I in large samples of sub-DLAs means that we will have a good indicator of α over Fe-peak element ratios.

Fig. 9 shows the evolution of the [O/Fe] ratio as a function of metallicity. All of these ratios are recomputed assuming $[O/H]_{\odot} = -3.26$ (Holweger 2001). In most cases, this ratio is subsolar at high metallicities ([Fe/H] > -1.6). However, [O/Fe] is still greater than solar at low metallicities. Similarly, Galactic metal-poor stars show an enhancement of between 0.35 and 1 (Goswami & Prantzos 2000 and references therein). However, in the case of high [O/Fe] ratio, one cannot decipher whether dust depletion or nucleosynthesis produces such high values. In the case of low [O/Fe], however, we know that the intrinsic values cannot be much smaller than the values observed.

Models from Hou et al. (2001) seem to underproduce the corresponding ratios with respect to the observations for both DLAs and sub-DLAs. In contrast, models from Calura et al. (2003) seem able to reproduce the observed subsolar values of [O/Fe] (see also Chiappini, Romano & Matteucci 2003). At present, however, the observed sample is still too small to allow firm conclusions to be drawn.

[C/Fe]. For the same reasons as O I, the first comprehensive set of measurements of C II has been made in high H I absorbers. [C/Fe] is approximately solar in the majority of the Galactic stars. Previous studies of DLAs only allowed for lower limit determinations (see Fig. 10), but measurements of C II in sub-DLAs provide a tracer of Fe-peak elements regardless of dust depletion. In this figure we use $[C/H]_{\odot} = -3.41$ (Holweger 2001) as an estimate of the solar value. Some of the [C/Fe] ratios in sub-DLAs are clearly oversolar, at the level of the overabundance observed in the two tentative [C/Fe] measurements in the DLAs. Since C is a mildly refracted element in the interstellar medium, these measurements provide our best indicator of the dust content of sub-DLAs. Indeed, although C and Fe do not share the same nucleosynthesis origin, in the Milky Way stars, C and Fe show identical behaviours, i.e. [C/Fe] $= 0$ (Goswami & Prantzos 2000). Therefore, the deviation from zero observed in sub-DLAs are suggestive of either the presence of dust in these systems or a different behaviour of C relative to Fe relative to the Milky Way stars. Both types of chemical evolution models predict abundance ratios in the intermediate range between DLAs and sub-DLAs. Nevertheless, the models of Hou et al. (2001) do not include yields from intermediate-mass stars. This will affect the [C/Fe] abundance ratio. The models of Calura et al. (2003) predict very little difference between DLAs and sub-DLAs, as is observed. However, again, given the limited data set, these conclusions are tentative.

[Al/Fe]. The metallicity evolution of the [Al/Fe] ratio is presented in Fig. 11, using $[Al/H]_{\odot} = -5.51$ (Grevesse & Sauval 1998). In DLAs, this ratio follows a trend similar to that observed in metal-poor stars (Prochaska & Wolfe 2002). In the sub-DLA case, this

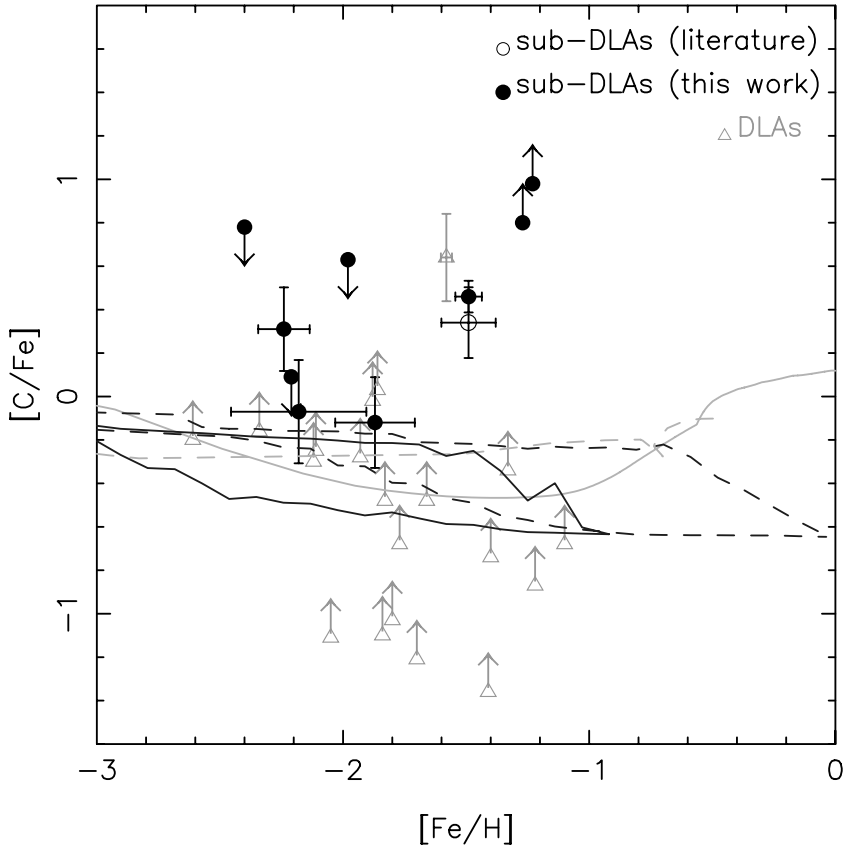

Figure 10. [C/Fe] ratio as a function of metallicity. Sub-DLAs are markedly more oversolar than DLAs. The dark-coloured solid (dashed) curves are contours for sub-DLAs (DLAs) column densities derived from models of disc galaxies (Hou et al. 2001). The light-coloured solid (dashed) curves are for spirals (irregulars) representative of sub-DLAs (DLAs) in the models of (Calura et al. 2003). This figure is available in colour in the online version of the journal on *Synergy*.

ratio is strongly affected by ionization corrections, which increase the real abundance of Al with respect to that measured solely from Al II. The [Al/Fe] ratio will consequently rise by a factor of 0.3 dex in the worst case (see Paper I). Again sub-DLAs are characterized by a mean [Al/Fe] elemental ratio larger than DLAs. In this case, we note that models of Hou et al. (2001) do not match the values of high-redshift DLAs nor the observations in the Milky Way. It should be noted that the nucleosynthesis situation of this element is unclear (Goswami & Prantzos 2000) but it could also be that the intermediate-mass stars not included in the models contribute to the true [Al/Fe] abundance ratio.

6 CONCLUSION

Péroux et al. (2003) have extended the DLA definition to a new class of absorbers: the sub-DLAs with column density $10^{19} < N(\mathrm{H\,I}) < 2 \times 10^{20}$ atom cm^{-2}. These systems are believed to contain a large fraction of the neutral gas mass in the Universe, especially at $z > 3.5$. Based on these considerations, we have constructed and fully analysed a sample of 12 sub-DLAs (see Paper I). In the present paper, we analyse several of the properties of these absorbers in conjunction with DLAs from the literature. Our main findings can be summarized as follows.

(i) Our sample of sub-DLAs can be used to observationally determine for the first time the shape of the column density distribution, $f(N)$, down to $N(\mathrm{H\,I}) = 10^{19}$ cm^{-2}. The results are in good agreement with the predictions from Péroux et al. (2003). An evolutionary study of $f(N)$ is not possible with the current sample illustrating the need for observations of sub-DLAs at high redshifts.

(ii) An analysis of the clustering of sub-DLAs in our sample shows that these are more clustered than expected from a random distribution, although the number statistic is too small to draw firm conclusions.

(iii) We measure the kinematic properties of the sub-DLAs from our sample together with a statistically significant number of DLAs from the literature. We compare low- and high-ionization transition widths and find that the sub-DLA properties roughly span the parameter space of the DLAs, thus challenging multicomponent semi-analytical models, such as that presented by Maller et al. (2002).

(iv) The metallicity of absorbers as traced by [Fe/H] shows a slightly more pronounced slope for sub-DLAs ($\alpha = -0.40 \pm 0.22$) than for DLAs ($\alpha = -0.18 \pm 0.12$). In addition, the HI-weighted mean metallicity is computed for various subsets of quasar absorbers. The evolution of $[\langle \mathrm{Fe/H_{DLA}} \rangle]$ might be stronger for sub-DLAs than for DLAs, and absorbers with $N(\mathrm{H\,I}) > 10^{21.0}$ atom cm^{-2} appear to be less evolved, suggesting these objects in particular should be studied in detail. Observational evidence supports the hypothesis that this different behaviour is *not* due to the hidden effect of dust. We therefore propose that sub-DLAs might be associated with a class of galaxies that better traces the overall chemical evolution of the Universe.

(v) A study of the metallicity evolution with metal line profile ionization width might show hints of a correlation, whereby higher

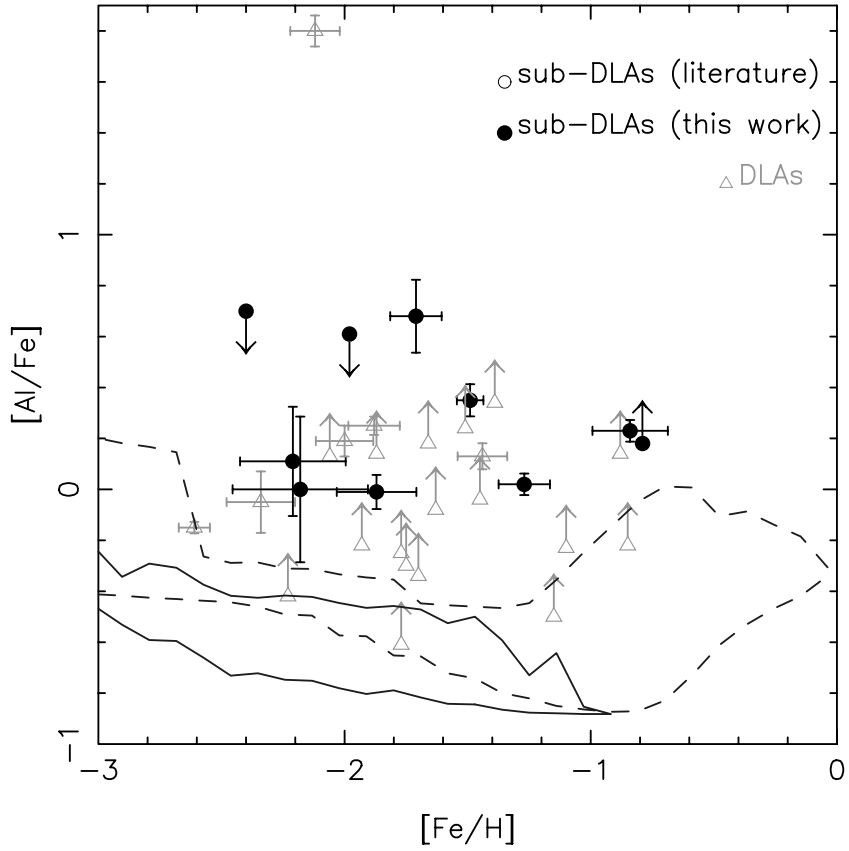

Figure 11. [Al/Fe] ratio as a function of metallicity. Again, sub-DLAs are remarkably more oversolar than DLAs. The solid (dashed) curves are contours for sub-DLAs (DLAs) column densities derived from models of disc galaxies (Hou et al. 2001). This figure is available in colour in the online version of the journal on *Synergy*.

[Fe/H] ratios are associated with systems with larger widths. However, the statistical significance of this result is low and a larger sample of observations is required to unambiguously address this issue.

(vi) Abundance ratios for [Si/Fe], [O/Fe], [C/Fe] and [Al/Fe] were determined and compared with two different sets of models of the chemical evolution of galaxies. Overall, these appear to resemble abundance ratios observed in DLAs. The question thus remains open as to whether the two classes of objects have similar chemical evolution histories or whether there are objects with different ages and star formation histories, but at a similar stage of chemical evolution. The first comprehensive sets of measurements of O I and C II in high H I column density systems are given. Indeed, these are well defined in sub-DLAs, while they are almost always saturated in DLAs. These elements, unaffected by dust depletion, provide direct indicators of the abundances in these systems.

These various issues illustrate the importance of further studies of sub-DLAs to interpret the overall chemical evolution of neutral matter with redshift, and to extend the analysis of quasar absorbers properties to a lower column density range. We are currently undertaking an observational programme aimed at studying sub-DLAs at high redshifts.

ACKNOWLEDGMENTS

We are grateful to Samuel Boissier for extending the predictions of Hou, Boissier & Prantzos (2001) to the sub-DLA column densities and to Francesco Calura for doing the same with the models of Calura, Matteucci & Vladilo (2002). We have benefited from conversations with Samuel Boissier, Francesco Calura, Mike Irwin, Ari Maller, Francesca Matteucci, Paolo Molaro, Nikos Prantzos, Simone Recchi and Zheng Zheng. We also thank an anonymous referee for extensive and helpful comments. This work was supported in part by the European Community Research and Training Network 'The Physics of the Intergalactic Medium'. CP is founded by an European Marie Curie Fellowship and MDZ by Swiss National Funds. RGM thanks the Royal Society.

REFERENCES

Bechtold J., 1994, ApJS, 91, 1
Boissé P., Le Brun V., Bergeron J., Deharveng J.M., 1998, A&A, 333, 841
Boissier S., Prantzos N., 1999, MNRAS, 307, 857
Boissier S., Prantzos N., 2000, MNRAS, 312, 398
Boissier S., Péroux C., Pettini M., 2003, MNRAS, 338, 131
Calura F., Matteucci F., Vladilo G., 2003, MNRAS, 340, 59
Cen R., Ostriker J.P., Prochaska J.X., Wolfe A.M., 2003, ApJ, submitted (astro-ph/0203524)
Chiappini C., Matteucci F., Gratton R., 1997, ApJ, 477, 765
Chiappini C., Romano D., Matteucci F., 2003, MNRAS, 339, 63
Corbelli E., Salpeter E., Bandiera B., 2001, ApJ, 550, 26
Dessauges-Zavadsky M., D'Odorico S., McMahon R.G., Péroux C., 2001, in Ferlte R., Lemoine M., Desert J.-M., Raban B., eds., 17th IAP Astrophysics Colloquium
Dessauges-Zavadsky M., Péroux C., Kim T.S., D'Odorico S., McMahon R.G., MNRAS, 2003, 345, 447 (Paper I)

D'Odorico V., Petitjean P., Cristiani S., 2002, A&A, 390, 13
Ellison S.L., Lopez S., 2001, A&A, 380, 117
Ellison S.L., Pettini M., Steidel C.C., Shapley A.E., 2001, ApJ, 549, 770
Gardner J.P., Katz N., Hernquist L., Weinberg D.H., 1997, ApJ, 484, 31
Goswami A., Prantzos N., 2000, A&A, 359, 191
Grevesse N., Sauval A.J., 1998, Space Sci. Rev. Vol. 85, Standard Solar Composition. Kluwer, Dordrecht, p. 161
Haehnelt M., Steinmetz M., Rauch M., 1998, ApJ, 495, 647
Holweger H., 2001, in Wimmer-Schweingruber R.F., ed., AIP Conf. Proc. Vol. 598, Joint SOHO/ACE workshop, Solar and Galactic Composition. Am. Inst. Phys. Woodbury, NY, p. 23
Hou J.L., Boissier S., Prantzos N., 2001, A&A, 370, 23
Kulkarni V.P., Fall S.M., 2002, ApJ, 580, 732
Lanzetta K., McMahon R.G., Wolfe A., Turnshek D., Hazard C., Lu L., 1991, ApJS, 77, 1
Ledoux C., Petitjean P., Bergeron J., Wampler J., Srianand R., 1998, A&A, 337, 51L
Lopez S., Ellison S.L., 2003, A&A, 403, 573
Lopez S., Maza J., Masegosa J., Marquez I., 2001, A&A, 366, 387
Maller A.H., Prochaska J.X., Somerville R.S., Primack J.R., 2001, MNRAS, 236, 1475
Maller A.H., Prochaska J.X., Somerville R.S., Primack J.R., 2002, MNRAS, 343, 268
Nagamine K., Springel V., Hernquist L., 2003a, MNRAS, submitted (astro-ph/0302187)
Nagamine K., Springel V., Hernquist L., 2003b, MNRAS, submitted (astro-ph/0305409)
Pei Y. C, Fall M.S., 1995, ApJ, 454, 69
Pei Y.C., Fall M.S., Hauser M.G., 1999, ApJ, 522, 604
Péroux C., Storrie-Lombardi L., McMahon R., Irwin M., Hook I., 2001, AJ, 121, 1799
Péroux C., Irwin M., McMahon R.G., Storrie-Lombardi L.J., 2002, in Fusco-Femiano R., Matteucci F., eds., ASP Conf. Proc. Vol. 253, Chemical Enrichment of Intracluster and Intergalactic Medium. Astron. Soc. Pac., San Francisco, p. 501
Péroux C., McMahon R., Storrie-Lombardi L., Irwin M., 2003, MNRAS, submitted (astro-ph/0107045)
Petitjean P., Srianand R., Ledoux C., 2000, A&A, 364L, 26
Petitjean P., Webb J., Rauch M., Carswell R., Lanzetta K., 1993, MNRAS, 262, 499
Pettini M., Smith L.J., King D.L., Hunstead R.W., 1997, ApJ, 486, 665
Pettini M., Ellison S.L., Steidel C.C., Bowen D.V., 1999, ApJ, 510, 576
Prantzos N., Boissier S., 2000, MNRAS, 315, 82
Prochaska J.X., Wolfe A.M., 1998, ApJ, 507, 113
Prochaska J.X., Wolfe A.M., 1999, ApJS, 121, 369
Prochaska J.X., Wolfe A.M., 2000, ApJ, 533, L5
Prochaska J.X., Wolfe A.M., 2002, ApJ, 566, 68
Prochaska J.X., Gawiser E., Wolfe A.M., 2001, ApJ, 552, 99
Prochaska J.X., Howk J.C., O'Meara J.M., Tytler D., Wolfe A.M., Kirkman D., Lubin D., Suzuki N., 2002, ApJ, 571, 693
Savaglio S., 2000, IAUS, 204, 24
Steidel C.C., Adelberger K.L., Dickinson M., Giavalisco M., Pettini M., Kellogg M., 1998, ApJ, 492, 428
Storrie-Lombardi L., Wolfe A., 2000, ApJ, 543, 552
Storrie-Lombardi L., Irwin M., McMahon R., 1996a, MNRAS, 282, 1330
Storrie-Lombardi L., McMahon R., Irwin M., 1996b, MNRAS, 283, L79
Vladilo G., Bonifacio P., Centurión M., Molaro P., 2000, ApJ, 543, 24
Wolfe A., Prochaska J.X., 2000a, ApJ, 545, 591
Wolfe A., Prochaska J.X., 2000b, ApJ, 545, 603
Wolfe A., Lanzetta K.M., Foltz C.B., Chaffee F.H., 1995, ApJ, 454, 698
Zheng Z., Miralda-Escudé J., 2002, ApJ, 568, 71

This paper has been typeset from a TEX/LATEX file prepared by the author.